COMMUNICATION

One-pot green synthesis of anisotropic silver nanoparticles†

Zeinab Hosseinidoust,‡[abc] Mohan Basnet,[a] Theo G. M. van de Ven[bc] and Nathalie Tufenkji*[a]

Anisotropic silver nanoplates are of interest for their shape-dependent properties; however, their synthesis often requires surfactants and toxic chemicals. We report the first one-pot method for the green synthesis of colloidally stable triangular, hexagonal and dendric silver nanostructures, enabled by the unique physical and chemical architecture of "hairy" cellulose nanocrystals (CNCs). Silver nanoplates were formed by irradiating a suspension of CNCs and silver nitrate in a UV chamber for as little as 5 min. Electron microscopy and diffraction analysis revealed that CNCs with low carboxyl content resulted in single crystal thin triangular nanoprisms. Increasing the CNC carboxyl content resulted in hexagonal nanosheets and flower-like/dendric structures. The synthesized nanoplates exhibited shape-dependent catalytic performance for methylene blue degradation.

Nano impact

Synthesis of anisotropic metallic nanoplates from metal salts often requires surfactants and toxic chemicals. Green agents such as polysaccharides have only been shown to achieve pseudospherical nanoparticles. We report the liquid-phase synthesis of silver nanoprisms without the need to use harsh chemicals and additives or seed particles, enabled by a novel preparation of "hairy" cellulose nanocrystals (CNCs). This is the only method to date that can synthesize a stable colloidal suspension of anisotropic silver nanoparticles simply by adding *a single agent* to the metal salt solution. This green method contributes to ongoing efforts for sustainable development of nanomaterials.

Decreasing the structural symmetry of silver nanoparticles can substantially influence their optical, electronic, catalytic and even biological properties, leading to new and advanced applications in surface plasmonics,[1] encryption technologies,[2] chemical/biological sensing,[3] antimicrobial surfaces,[4] and high performance catalysis.[5] The preparation of nanostructures with different controlled shapes is an effective route to fine-tune their chemical and physical properties with a greater versatility than can be achieved otherwise.[6] For example, triangular/plate-like nanostructures are of interest for their structure- and environment-dependent optical features and their anisotropic surface energetics.[7,8] Although the experimental details differ amongst the various

methods for preparing plate-like nanostructures, most of these methods are based on two-step, seed-mediated reduction (Table S1†). None of these methods are regarded as being green due to the presence of harsh chemicals and additives.[9] Polysaccharides such as cellulose can be used for green synthesis of metal nanoparticles.[10–12] However, polysaccharides have not been successfully used for producing anisotropic metal nanoparticles or achieving shape control.

We report a simple single-step, green method for the synthesis of silver nanoplates with different shapes based on UV photoreduction of a silver salt in the presence of cellulose nanocrystals (CNCs). CNCs are rod-shaped nanoparticles isolated from cellulosic biomass by chemically removing the amorphous regions in cellulose fibers, leaving the highly ordered crystalline regions intact (Scheme S1a and b†).[13] We previously reported a two-step oxidation process to produce "hairy" CNCs flanked by a soft, porous layer of dicarboxylic cellulose (DCC) chains (Scheme S1c†),[14] yielding nanocrystals with a remarkably high number of carboxyl groups.[15,16] The surface charge of the CNCs can be tuned by acid cleavage of the DCC chains to various extents (Scheme S1c†).[17] In the proposed method for synthesis of silver nanostructures, CNCs act simultaneously as mediators for differential crystal growth and shape control as well as metal cation nucleation sites, redox agent, capping agent and stabilizer. This technique is one

[a] *Department of Chemical Engineering, McGill University, Montreal, Quebec H3A 0C5, Canada. E-mail: nathalie.tufenkji@mcgill.ca; Fax: +(514) 398 6678; Tel: +(514) 398 2999*

[b] *Department of Chemistry, McGill University, Montreal, Quebec H3A 2K6, Canada*

[c] *Pulp & Paper Research Centre, McGill University, Montreal, Quebec H3A 2A7, Canada*

† Electronic supplementary information (ESI) available: Table S1 and Figures S1 to S9. See DOI: 10.1039/c6en00112b

‡ Current affiliation: Department of Chemical Engineering, McMaster University, Hamilton, ON, Canada.

This journal is © The Royal Society of Chemistry 2016

Environ. Sci.: Nano, 2016, 3, 1259–1264 | 1259

of the very few non-plasmonic methods and the only green method that can alter the shape of metallic nanostructures without the use of seed particles, harsh chemicals, and surfactants. We further demonstrated the shape-dependent catalytic performance of the silver nanoparticles for degradation of methylene blue.

Results and discussion

Three samples of CNCs having different carboxyl contents (Table 1) were prepared as previously reported.[17] CNCs were ~100 nm in length and ~5 nm in diameter, as determined from TEM images (Fig. 1a, Table 1); however, the presence of the long DCC chains on the poles resulted in a larger hydrodynamic diameter in deionized water (DI) for samples CNC-1 and CNC-2, as measured by dynamic light scattering (Table 1).

Each CNC sample was mixed with a solution of silver nitrate (final concentration of 0.5 mM) and immediately irradiated at 254 nm (4.6 mW cm^{-2}) for various lengths of time. The initial colorless mixture turned to pale yellow after only 5 min of irradiation, with the color changing to different shades of dark yellow, orange and red with increasing time. The molar ratio of carboxyl groups to Ag$^+$ ranged from 25 for the CNC sample with high carboxyl content (CNC-1), to 4 for the CNC sample with low carboxyl content (CNC-3). The suspensions were stable during a 10 month monitoring period with negligible color change and no trace of precipitate formation (Fig. 1b). No color change was observed for mixtures of AgNO$_3$ and CNCs in the absence of UV treatment, even after several days of exposure to fluorescent lighting or prolonged incubation at 40 °C (Fig. S1†). UV treatment of AgNO$_3$ mixed with non-carboxylated cellulose (i.e., Avicell microcrystalline cellulose beads or CNCs prepared from wood pulp via hydrolysis by HCl) showed no color change (Fig. S1†) or SPR peak (Fig. S2†) even after longer periods of UV treatment. These results are summarized in Table 2. Extinction spectra for AgNO$_3$/CNC mixtures subjected to UV treatment exhibited a visible secondary peak after 30 min of UV treatment, with the intensity of the peaks gradually increasing, and a clear red shift which is associated with the presence of anisotropic silver nanostructures (Fig. 1c and d). Interestingly, the peaks did not broaden with time, suggesting that the size distribution of nanoparticles was preserved during UV treatment. This could also indicate that the kinetics of nanoparticle formation is faster than the time resolution of our observations, which is supported by the observation that 5 min of treatment was sufficient to produce a
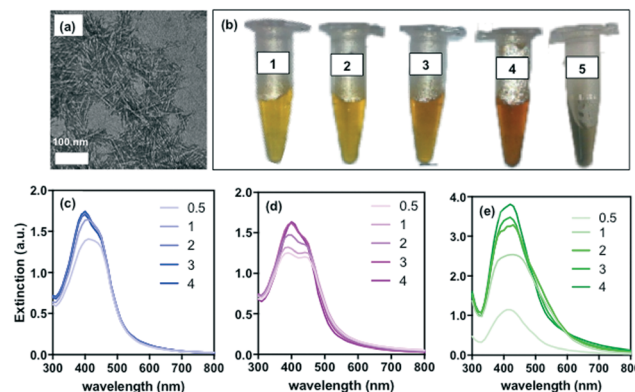

Fig. 1 (a) Transmission electron micrograph of sample CNC-1. (b) Photographs of colloidal dispersions of silver nanoparticles synthesized with (1) CNC-1, 30 min UV treatment, (2) CNC-2, 30 min UV treatment, (3) CNC-3, 30 min UV treatment, (4) CNC-3, 1 h UV treatment, (5) rhamnolipids, 30 min UV treatment. Images were recorded after 10 months of storage at room temperature. Note the thick layer of silver precipitate formed in sample 5. Extinction spectra measured after different durations of UV treatment for a mixture of AgNO$_3$ with (c) CNC-1, (d) CNC-3, and (e) rhamnolipids.

color change, indicative of nanosilver formation. For comparison, a mixture of AgNO$_3$ and rhamnolipids (a carboxyl-rich biosurfactant) was subjected to the same UV treatment. This system produced a markedly different extinction spectra (no secondary peak), suggesting slower kinetics and a change in particle size distribution with time (Fig. 1e). Furthermore, the resulting suspension was not stable for a long period when exposed to light (Fig. 1b).

TEM micrographs revealed that CNCs with a higher carboxyl content (CNC-1) led to the formation of flower-like or dendric structures (Fig. 2a and b) with a lattice parameter of ~0.54 nm (Fig. 2c). Decreasing the carboxyl content of the CNCs resulted in the formation of single crystal hexagonal plates for CNC-2 (Fig. 2d and e). CNC-3 (the sample with the lowest carboxyl content) resulted in triangular plates (Fig. 2f) composed of a mixture of whole triangles, triangles with rounded vertices and triangles with small truncation at vertices, as reported previously for other synthesis techniques.[9] Fig. S3† shows lower magnification micrographs of the synthesized silver structures. What is clear from Fig. S3† is the markedly low (<10%) population of spherical nanoparticles. The smaller, seemingly spherical, particles exhibit anisotropic growth with increased reaction time. This phenomenon can be partially attributed to the non-homogeneous nature of the reaction across the reaction volume due to the lack of mixing and is discussed in detail further along in the manuscript.

The control (rhamnolipid system) resulted in pseudo-spherical nanoparticles (Fig. 2g) that appeared as multiple islands on the TEM grid (a hallmark of nanoparticle aggregation upon drying), while the CNC system resulted in well-dispersed nanostructures when dried on the TEM grid. This observation, along with the exceptionally high colloidal stability of the CNC-nanosilver suspensions suggests that the

Table 1 Characterization of CNC samples

Sample	–COOH content (mmol g^{-1})	Hydrodynamic diameter (nm)	TEM size (nm), length–width
CNC-1	6.6	234 ± 4	97 ± 8–4 ± 2
CNC-2	3.8	219 ± 4	103 ± 2–6 ± 1
CNC-3	1.7	125 ± 7	107 ± 1–7 ± 2

Table 2 Summary of results for silver nanoparticle formation under different conditions

Agents added to $AgNO_3$ (0.5 mM)	With UV treatment	Without UV treatment
CNC-1	++	−
CNC-2	++	−
CNC-3	++	−
CNC-1, degassed	++	−
CNC-1, UV treated for 30 min	NA	+
CNC-3, UV treated for 30 min	NA	+
CNC (not carboxylated)	−	−
DCC	+	−
Avicell microcrystalline cellulose beads (MCC)	−	−
Rhamnolipids	++	−
None	−	−

++: intense color change observed; +: slight color change observed; −: no color change.

silver nanostructures may form a hybrid with the CNCs, and thus benefit from their high colloidal stability. This hypothesis, however, remains to be confirmed as the CNCs are difficult to visualize by TEM without negative staining. Selected area electron diffraction (SAED) revealed that the nanostructures formed by CNC-2 and CNC-3 crystallized in face-centered cubic (fcc) system along the [111] zone axis (Fig. 2h and i), which is consistent with that reported in the literature.[18,19] Energy-dispersive X-ray spectroscopy (EDS) confirmed the presence of elemental silver in all cases (Fig. S4†). TEM image analysis revealed that the size of the silver nanostructures varies between 50–200 nm, with most particles in the size range of 100–150 nm for CNC-1 and CNC-2, and 70–110 nm for CNC-3 (Fig. S5†).

As a demonstration of the potential application of the synthesized nanostructures, each population was employed as the catalyst in reduction of methylene blue, a model dye degradation reaction. The extent of dye degradation was quantified by measuring the absorption of the reaction mixture at 664 nm. Fig. S6† shows that all three nanostructure populations exhibit different catalytic activity, with the triangular and hexagonal nanoplates showing superior activity compared to the dendric structures. All three groups of nanoparticles synthesized in the presence of CNCs show superior catalytic performance to that of the control group; namely, pseudospherical nanoparticles synthesized *via* photoreduction in the presence of rhamnolipids instead of CNCs.

Cellulose and CNCs were previously used as substrates for nanoparticle synthesis (*via* chemical,[20] thermal[21] or UV-mediated reduction[22]). UV photon absorption can break the oxygen bridge between the glucose monomers in a cellulose chain, forming chemical species[23,24] that can reduce Ag^+ ions. Carboxylation of cellulose is known to increase its sorptive properties for metal ions;[25–27] therefore the highly carboxylated CNCs could act as a strong nucleation site for metal cations, increasing the rate of nanoparticle synthesis. However, there has been no report of cellulose or other polysaccharides playing any role in the synthesis of anisotropic metallic structures and, thus, the mechanism of shape control remains to be investigated. We hypothesized that the specific physical structure of the CNCs used in this work, namely the amorphous DCC chains on the poles, and their controllable charge density, may be responsible for the formation of different shapes of nanosilver. To validate this hypothesis, CNCs were UV treated for 30 min to activate/cleave the DCC chains (since amorphous cellulose is more susceptible to chemical reactions compared to crystalline cellulose[13]) before being mixed with $AgNO_3$. No color change was observed after addition of the metal salt precursor and incubation at room temperature (Fig. S1†). However, with longer incubation (up to 4 h, in dark or exposed to light), a very pale color developed (Fig. S7†). Extinction spectra showed a weak SPR peak for $AgNO_3$/CNC-2 and $AgNO_3$/CNC-3, whereas $AgNO_3$/CNC-1 presented a noticeable and broad peak at ~400 nm (Fig. S8a and b†). TEM images of the $AgNO_3$/CNC-1 sample revealed
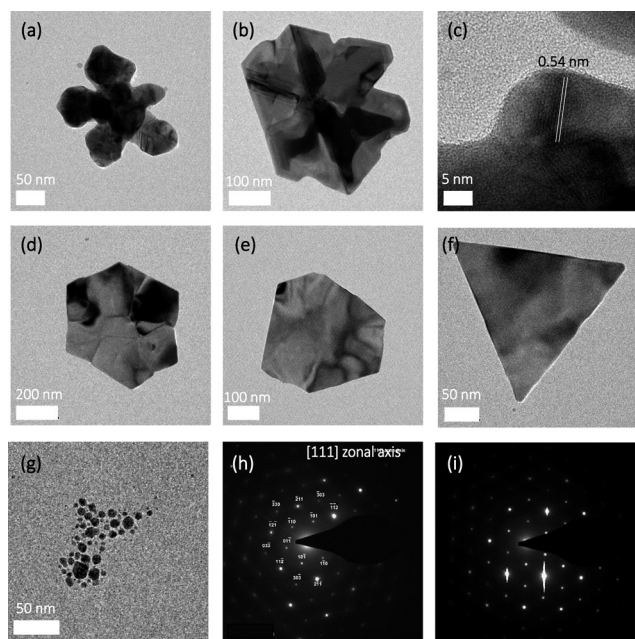

Fig. 2 Transmission electron micrographs of silver nanoplates prepared by a 30 min UV treatment of $AgNO_3$ with (a–c) CNC-1, (d, e) CNC-2, (f) CNC-3, and (g) rhamnolipids. Panel (c) shows the crystal plane spacing for the nanostructure in (b). (h) Electron diffraction of silver nanoplate in (e). (i) Electron diffraction of silver nanoplate in (f).

This journal is © The Royal Society of Chemistry 2016

Environ. Sci.: Nano, 2016, **3**, 1259–1264 | **1261**

highly polydisperse fractal silver structures (Fig. 3a) with the smaller structures (Fig. 3b and c) bearing resemblance to the fractal flower-like structures observed in Fig. 2a and b. Similar structures were observed with CNC-2 and CNC-3, albeit at a much lower density (Fig. 3d and e). The structures formed exhibit a polycrystalline nature (Fig. 3f); however, the larger silver structures contained large segments of single crystals (Fig. 3g). These observations suggest that UV activation of CNCs produces redox species (either by creating reactive species on the cellulose sugar rings or by cleavage of DCC chains) that can reduce silver ions upon addition of silver salt to the radiated CNC suspension. However, in the absence of UV radiation, the energy in natural light is insufficient to sustain redox species and, thus, silver is formed on the surface of already formed structures instead of forming new nanoparticles. This observation confirms that UV activation of the CNCs drives the formation of silver nanostructures with complex shapes.

To confirm the role of the DCC chains, pure dicarboxylated cellulose (without CNCs[14]) was mixed with AgNO$_3$ and UV-treated for 30 min. A pale color change was observed (Fig. S1†). The TEM analysis showed a very low density of pseudospherical nanoparticles with very few triangular prisms observed after 4 h of UV treatment (Fig. 3h). Carboxylate-rich polymers are effective photoreduction agents for metal cations. The high-density of DCC chains on the poles of the CNC nanorods likely provides a more efficient site for the accumulation of the silver cations compared to the dispersed

DCC chains in this experiment, thus explaining the slow kinetics and low yield in the dispersed DCC system.

The mechanism driving the formation of different plate-like structures in the presence of CNCs remains to be elucidated. It is believed that one of the factors affecting the final shape of a nanoparticle is twinning, *i.e.*, surface energetics driven accumulation of faults in the crystal structure during the initial phases of nanoparticle formation.[28] The morphology of this initial seed particle can determine the structure of the ultimate anisotropic particle by limiting the number and variety of crystal facets available for growth.[29] Electron micrographs of AgNO$_3$/CNC mixtures after 5–10 min of UV radiation revealed the presence of nanoparticles that appeared to deviate from spherical structures (Fig. S9†), which may indicate the early introduction of faults in the crystal structure. Interestingly, it has been shown for nanoparticles of AgBr that even when they look spherical, on the atomic scale they are bound by the (111) and (100) faces.[30] This information must be interpreted with caution because the shape of small nanoparticles (<5 nm) can vary, and studying their morphology and crystal structure can be difficult. Furthermore, it is difficult to predict what nanoparticle morphology will lead to plate-like crystal growth and this information is not available in the literature. Even if we entertain the notion that stacking faults are responsible for the formation of different shapes, the question still remains as to the factors that drive the formation of twin planes in the presence of CNCs with differing surface charge. Presence of certain ions (*e.g.*, halides) is known to affect fault stacking and twinning planes,[31] and so it is likely that the products of UV activation/decomposition of cellulose chains could affect the stacking of the silver atoms during the initial stages of nanoparticle formation. Based on this theory, UV affects both reduction and shape control. The confirmation of this hypothesis, however, requires more in-depth investigation.

Experimental methods

Silver nanoparticle synthesis

Silver nitrate powder (Sigma-Aldrich) was used to prepare a 10 mM solution in DI water. The solution was then diluted to 1 mM in DI water and mixed 1:1 with different CNC samples. A fresh silver nitrate solution was prepared for each experiment. The mixture of silver salt and CNCs was immediately irradiated in a ProCleanerTM UV chamber (Nanoforce Biosciences, IA) at 254 nm (4.6 mW cm^{-2}) for various lengths of time, after which aliquots of the samples were taken and analyzed *via* a UV-vis spectrophotometer or TEM. Microcrystalline cellulose (50 μm, Avicell) was used as a pure non-derivatized form of cellulose, as control.

Extinction spectra

The spectral response of silver nanoparticles was measured using UV-visible spectroscopy. UV-visible spectra were recorded at room temperature using a spectrophotometer (Agilent HP Model 8453), with a 1 cm path length quartz
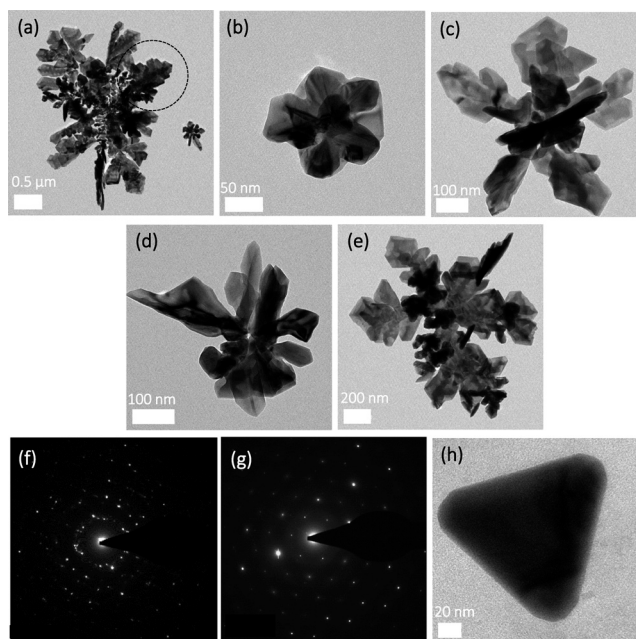

Fig. 3 Transmission electron micrographs of silver structures prepared by mixing different CNC samples that were UV-treated for 30 min with AgNO$_3$. (a–c) TEM images for CNC-1, (d) CNC-2, and (e) CNC-3. (f) SAED pattern for the polycrystal in panel (c), (g) SAED pattern for the single crystal marked in panel (a). (h) TEM image of silver nanoprism formed by 4 h UV treatment of a mixture of silver nitrate and DCC.

cuvette and a fixed slit width of 2 nm. Silver nanoparticles were analysed in the reaction medium (DI water) without further purification.

Preparation of cellulose nanocrystals

CNCs were prepared based on the method of Yang et al.[14] with key modifications to allow for tunable control of surface charge, as previously described in detail.[17]

Conductometric titration

Conductometric titrations were performed on a Metrohm 836 Titrando instrument. A volume of CNC suspension containing 0.02 g CNCs was diluted to 200 mL with DI water. The ionic strength of the suspension was adjusted using NaCl solution (to 0.28 mM) and pH was adjusted to 3.5 using 0.1 M HCl. The mixture was titrated with a 10 mM NaOH solution at a rate of 0.1 mL min^{-1}. The part of the titration curve representing weak acid titration (negligible change in conductivity with time) was used to calculate the carboxyl content.

Dynamic light scattering (DLS)

DLS measurements for CNCs were performed using a Malvern Instruments Zetasizer Nano-ZS. The samples were diluted to 0.1 wt% in DI and filtered using a 0.45 μm syringe filter. Standard quartz cuvettes were used for all measurements and each measurement was repeated five times at room temperature.

Transmission electron microscopy (TEM)

A glow-discharged carbon coated copper grid was placed on a 5 μL drop of CNC (0.1 w/w%) or silver nanoparticles for 5 min and washed 3 times by placing on drops of DI water for 10 s. For CNCs, the grids were negative stained using 2% uranyl acetate. All samples were examined via a Philips Tecnai 12 200 kV TEM and images were captured with a Gatan 792 Bioscan 1k × 1k Wide Angle Multiscan CCD Camera. SAED was performed with the same system operated at 200 kV and a camera distance of 240 mm. For measuring particle size using TEM, 30 images were captured from each sample and at least 50 particles were measured in each captured micrograph using ImageJ.

Catalytic degradation of methylene blue

The catalysis experiments were conducted as described in the literature.[32] Briefly, the suspension of silver nanostructures (0.4 mL) was added (immediately after preparation) to 11 mL of a mixture of sodium borohydride solution (9 mM) and methylene blue (18.2 mg L^{-1}). The mixture was continuously stirred using a magnetic stirrer for 2 min. The degradation of dye was quantified by measuring the absorbance of the reaction mixture at 664 nm every five min using a UV-vis spectrophotometer (Agilent HP Model 8453). The specific reaction rate for dye degradation was calculated by numerically calculating the slope of the methylene blue concentration profile and dividing by the catalyst surface area. The catalyst surface area was estimated using the size distribution data and the surface area of equilateral triangles, hexagons, and five sided stars for CNC-3, CNC-2, and CNC-1, respectively.

Conclusions

In summary, we present a one-pot green method for the preparation of different shaped plate-like silver nanostructures based on the surface density of carboxyl groups on CNCs. This synthesis employs CNCs dispersed in water as the only agent added to a metal salt precursor and, thus, presents a green approach for preparation of nanoparticles with various shapes. It is noteworthy that although our method allows for shape-control over the majority of the population, a small population of pseudo-spherical nanoparticles is present in all samples. Precise shape control over the entire reaction volume requires meticulous control and fine-tuning of reaction parameters and goes hand in hand with a deeper understanding of the mechanism that drives the development of the different shapes in the presence of hairy CNCs. Ongoing work in our laboratory is exploring the mechanism behind the formation of different shapes and application of this method to other metal salts (e.g., gold, platinum, zinc). The remarkable colloidal stability of the CNCs translates to a highly stable suspension of nanostructures, increasing their shelf-life and further expanding the range of applications of the nanoparticles to instances involving high ionic strength and complex fluids. This work is part of an ongoing effort for sustainable development of nanomaterials; ongoing studies in our laboratory are aimed at evaluating the catalytic, antimicrobial and other properties of the synthesized nanoplates.

Acknowledgements

Notes and references

1 Y. C. Cao, R. Jin and C. A. Mirkin, Science, 2002, 297, 1536–1540.

2 M. J. Banholzer, K. D. Osberg, S. Li, B. F. Mangelson, G. C. Schatz and C. A. Mirkin, ACS Nano, 2010, 4, 5446–5452.

3 D. G. Georganopoulou, L. Chang, J. M. Nam, C. S. Thaxton, E. J. Mufson, W. L. Klein and C. A. Mirkin, Proc. Natl. Acad. Sci. U. S. A., 2005, 102, 2273–2276.

4 M. R. Nateghi and H. Hajimirzababa, J. Text. Inst., 2014, 105, 806–813.

5 X. Lou, H. Pan, S. Zhu, C. Zhu, Y. Liao, Y. Li, D. Zhang and Z. Chen, Catal. Commun., 2015, 69, 43–47.

This journal is © The Royal Society of Chemistry 2016

Environ. Sci.: Nano, 2016, 3, 1259–1264 | 1263

6   T. K. Sau and A. L. Rogach, *Complex-shaped Metal Nanoparticles: Bottom-Up Syntheses and Applications*, John Wiley & Sons, 2012.

7   C. Burda, X. Chen, R. Narayanan and M. A. El-Sayed, *Chem. Rev.*, 2005, **105**, 1025–1102.

8   Y.-C. Yang, H.-J. Wang, J. Whang, J.-S. Huang, L.-M. Lyu, P.-H. Lin, S. Gwo and M. H. Huang, *Nanoscale*, 2014, **6**, 4316–4324.

9   J. E. Millstone, S. J. Hurst, G. S. Métraux, J. I. Cutler and C. A. Mirkin, *Small*, 2009, **5**, 646–664.

10 S. Padalkar, J. R. Capadona, S. J. Rowan, C. Weder, Y. H. Won, L. A. Stanciu and R. J. Moon, *Langmuir*, 2010, **26**, 8497–8502.

11 P. Raveendran, J. Fu and S. L. Wallen, *J. Am. Chem. Soc.*, 2003, **125**, 13940–13941.

12 M. Kaushik, A. Y. Li, R. Hudson, M. Masnadi, C.-J. Li and A. Moores, *Green Chem.*, 2016, **18**, 129–133.

13 R. H. Marchessault, F. F. Morehead and N. M. Walter, *Nature*, 1959, **184**, 632–633.

14 H. Yang, M. N. Alam and T. G. M. van de Ven, *Cellulose*, 2013, **20**, 1865–1875.

15 S. Safari, A. Sheikhi and T. G. M. van de Ven, *J. Colloid Interface Sci.*, 2014, **432**, 151–157.

16 A. Sheikhi, H. Yang, M. N. Alam and T. G. M. van de Ven, *J. Visualized Exp.*, 2016, (113), e54133, DOI: 10.3791/54133.

17 Z. Hosseinidoust, M. N. Alam, G. Sim, N. Tufenkji and T. G. van de Ven, *Nanoscale*, 2015, 16647–16657, DOI: 10.1039/c5nr02506k.

18 R. Jin, Y. Cao, C. A. Mirkin, K. L. Kelly, G. C. Schatz and J. G. Zheng, *Science*, 2001, **294**, 1901–1903.

19 A. Sarkar, S. Kapoor and T. Mukherjee, *J. Colloid Interface Sci.*, 2005, **287**, 496–500.

20 S. Padalkar, J. R. Capadona, S. J. Rowan, C. Weder, R. J. Moon and L. A. Stanciu, *J. Mater. Sci.*, 2011, **46**, 5672–5679.

21 S. Chen and D. L. Carroll, *Nano Lett.*, 2002, **2**, 1003–1007.

22 A. A. Omrani and N. Taghavinia, *Appl. Surf. Sci.*, 2012, **258**, 2373–2377.

23 J. B. G. A. Havermans and J. Dufour, *Restaurator*, 1997, **18**, 103–114.

24 M. Yatagai and S. H. Zeronian, *Cellulose*, 1994, **1**, 205–214.

25 X. Yu, S. Tong, M. Ge, L. Wu, J. Zuo, C. Cao and W. Song, *J. Environ. Sci.*, 2013, **25**, 933–943.

26 A. Sheikhi, S. Safari, H. Yang and T. G. M. Van De Ven, *ACS Appl. Mater. Interfaces*, 2015, **7**, 11301–11308.

27 A. W. Carpenter, C.-F. de Lannoy and M. R. Wiesner, *Environ. Sci. Technol.*, 2015, **49**, 5277–5287.

28 C. Lofton and W. Sigmund, *Adv. Funct. Mater.*, 2005, **15**, 1197–1208.

29 M. Liu and P. Guyot-Sionnest, *J. Phys. Chem. B*, 2005, **109**, 22192–22200.

30 B. Wiley, Y. Sun and Y. Xia, *Langmuir*, 2005, **21**, 8077–8080.

31 B. J. Wiley, Y. Xiong, Z.-Y. Li, Y. Yin and Y. Xia, *Nano Lett.*, 2006, **6**, 765–768.

32 V. S. Suvith and D. Philip, *Spectrochim. Acta, Part A*, 2014, **118**, 526–532.